Alternative approach for reproducing the in-plane behaviour of rubble stone walls

Nicola Tarque*[1a], Guido Camata[2b], Andrea Benedetti[3c] and Enrico Spacone[2d]

[1]*Division of Civil Engineering, Pontificia Universidad Católica del Perú, Av. Universitaria 1801, Lima, Peru*
[2]*Department of Engineering and Geology, University G. D'Annunzio, Viale Pindaro 42, Pescara, Italy*
[3]*Department of Civil, Chemical, Environmental, and Materials Engineering, University of Bologna, Via Zamboni 33, Bologna, Italy*

Abstract. Stone masonry is one of the oldest construction types due to the natural and free availability of stones and the relatively easy construction. Since stone masonry is brittle, it is also very vulnerable and in the case of earthquakes damage, collapses and causalities are very likely to occur, as it has been seen during the last Italian earthquake in Amatrice in 2016. In the recent years, some researchers have performed experimental tests to improve the knowledge of the behaviour of stone masonry. Concurrently, there is the need to reproduce the seismic behaviour of these structures by numerical approaches, also in consideration of the high cost of experimental tests. In this work, an alternative simplified procedure to numerically reproduce the diagonal compression and shear compression tests on a rubble stone masonry is proposed within the finite element method. The proposed procedure represents the stone units as rigid bodies and the mortar as a plastic material with compression and tension inelastic behaviour calibrated based on parametric studies. The validation of the proposed model was verified by comparison with experimental data. The advantage of this simplified methodology is the use of a limited number of degrees of freedom which allows the reduction of the computational time, which leaves the possibility to carry out parametric studies that consider different wall configurations.

Keywords: stone masonry; numerical modelling; finite element; experimental tests

1. Introduction

Stone masonry has been used for construction around the world since earliest civilization time. For example, early European populations such as the Greeks and the Romans used stone as decorative and structural elements. Later, in the middle ages the work by Gothic builders leads to more complex and slender structures, such as abbeys and castles. Remarkable examples of stone constructions are also those of the ancient Egyptians with their pyramids and the Persians with their temples and palaces. In Central America the use of stone is found in the Step Pyramids while in South America stone structures were used in fortresses and entire cities built by the Inca's Empire.

As part of the seismic risk mitigation and heritage conservation efforts, some researchers have evaluated the seismic performance and vulnerability of historical and vernacular stone masonry structures, especially structures placed in Europe, Middle East and Asia (Doğangün and Sezen 2012, Ural 2013, Seker et al. 2014, Karantoni et al. 2014, Gautam et al. 2016). Other researchers have studied how to numerically approach the dynamic behaviour of stone structures, using, mechanical models, finite element and discrete element methods Pere et al. 2005, Milosevic et al. 2013a, Lagomarsino et al. 2013). However, numerical analyses of stone masonry still remain an important task because of the limited experimental data available, the wide variations of mechanical properties of stone walls constituents (especially in the mortars, Pagnini et al. 2011, Doğangün and Sezen 2012,

*[a] Corresponding author, Ph.D., Associate Professor, sntarque@pucp.edu.pe
[b] Ph.D., Associate Professor, g.camata@unich.it
[c] Ph.D., Professor, andrea.benedetti@unibo.it
[d] Ph.D., Professor, espacone@unich.it

Karantoni et al. 2014), and the brittle behaviour of the stone walls.

Therefore, the objective of this work is to propose a simplified methodology to reproduce the in-plane behaviour of rubble stone single leaf walls. In this methodology the stones are treated as rigid body elements with three degrees of freedom (DOFs) while the mortar is treated within the plasticity theory using a plastic-damage model. This model characterizes the elastic and inelastic part of the mortar through its compression and tension constitutive law. To validate the methodology, some experimental diagonal compression tests and shear compression tests -carried in previous researches- were numerically reproduced here. The modelling approach was able to save computational time while retaining good accuracy in the numerical prediction of the wall mechanical response.

2. Review of some experimental tests and numerical modelling to evaluate stone masonry

2.1 Experimental tests

The principal objective of the experimental tests is to identify the mechanical properties that define the compression, tension and shear behaviour of the stone masonry (including stone and mortar) and to understand the global seismic behaviour of these type of constructions. The structural capacity of stone walls can be assessed through pseudo static monotonic and cyclic tests, while the complete dynamic behaviour of the stone construction can be identified through dynamic tests on full or scaled specimens. Some experimental tests have enhanced the knowledge of the mechanical properties of stone masonry (e.g. Valluzi et al. 2001, Corradi et al. 2003, Vasconcelos 2005, Binda et al. 2006, Frumento 2007, Gardin 2007, Dolce et al. 2008, Vasconcelos and Lourenço 2009, Oliveira et al. 2012, Milozevic et al. 2012, Vintzileou 2015, Graziotti et al. 2016, Spacone 2016).

According to literature two basic in-plane failure modes can occur at the level of the stone-mortar interface for the stone masonry: tensile failure associated to stresses acting normal to the joints that lead to interface separation and shear failure corresponding to a sliding mechanism of the units or shear failure of the mortar joint. Vasconcelos (2005) investigated the properties of granites to characterize the units and the mortar and the interaction between them by means of tensile, compressive and shear experimental tests. Furthemore, in-plane cyclic tests were performed on three typologies of single leaf stone masonry: dry-stone masonry, irregular stone masonry and rubble stone masonry. Oliveira and Lourenço (2006) tested multi-leaf stone walls made of roughly shaped granite stones bonded with lime-based mortar and aligned bed joints, these multi-leaf walls did not have transversal connections. They concluded that the typical failure started with out-of-plane displacements of the external leaves, due to the development of horizontal plastic hinges, and shifted to the formation of a dominant vertical cracking pattern and the localized loss of equilibrium at some stone units. Milosevic et al. (2013b) carried out tests to evaluate the most important mechanical parameters for numerical modelling of stone masonry as Young's modulus, cohesion and friction coefficient and tensile strength. They performed 2 compression tests, 9 triplet tests and 4 diagonal compression tests on stone masonry and using two types of mortar: air and hydraulic lime mortar, to simulate different construction periods. These walls were built using traditional Portuguese techniques to represent typical Lisboan buildings. Corradi et al. (2003) carried out an experimental study on the strength properties of double-leaf roughly cut stone walls by means of in-situ simple compression, diagonal compression and shear-compression tests. The masonry walls were

representative of buildings in Umbria, Italy. They found that the variability of the mechanical property values, more specifically those of the elastic and shear moduli, depends on the masonry typology. Similar experimental tests on rubble stone masonry from Italy can be found, among others, in Frumento (2007), Dolce et al. (2008), Magenes et al. (2010, 2014) and recently Graziotti et al. (2016) and Spacone (2016). This last focused on monotonic and shear-compression tests on small specimen representative of typical Abruzzo's wall.

2.2 Numerical modelling approach

The numerical analysis of masonry constructions is not an easy task, normally the structure involves geometrical complex, non-linearity of the material and interaction among them (bricks and mortar joints), and different local failure mechanisms, which ends in a large computational effort in case of a finite element model (Mazzon 2010, Roca et al. 2005). Regarding all numerical methodologies, three main classification may be individuated: limit analysis, equivalent frame modelling, and finite element modelling.

In the limit analysis, the failure of the structure is given by assuming certain failure mechanisms -given by the rotation of rigid blocks- to compute the load capacity. Therefore, the failure should be known a priori in order to draw the separated blocks. Although this methodology has been implemented to 3D models, the main limitation is the no representation of local failures. The main assumptions of this method is that material has not tensile strength, it has infinitive compressive strength, sliding failure does not occur and just small displacement is allowed.

In the equivalent frame model, each wall (pier) and lintel beam (spandrel) is represented by a frame, where each frame is connected at the ends to each other by rigid arms (Lagomarsino et al. 2013, Penna et al. 2016). Nonlinear flexural springs (lumped plasticity) are also inserted at the frame ends and translational shear springs at the mid-frame to take into account the non-linearity of the composite. The advantage of this method is the accuracy to reproduce the global behaviour (3D) of masonry buildings and the reasonable computation effort; however, it cannot model as well local failure modes as out-of-plane failure.

Finite element method (FEM) using calibrated stress-strain relationships represents a suitable numerical approach to reproduce the masonry behaviour (Tarque et al. 2013). The level of accuracy in the numerical models strongly depends on the knowledge of the material properties, the type of analyses (e.g. linear, nonlinear), the finite elements used (e.g. shell elements, brick elements), and the solution scheme adopted (e.g. implicit or explicit, Pelá et al. 2013, Tarque et al. 2014, Seker et al. 2014). Previous research results have shown that the response of masonry structures up to failure can be successfully modelled using techniques applied to concrete mechanics within the FEM (Pelà et al. 2013), because the material is brittle in tension with exponential energy lost. According to Lourenço (1996), the numerical modelling of masonry walls can generally follow either the micro-modelling of each of its components (discontinuous or discrete approach) or the macro-modelling of the wall (continuum approach), thus assuming that the masonry wall is homogeneous. The former can be divided into:

- detailed-micro modelling. Bricks and mortar joints are discretized using continuum elements, with the brick-mortar interface represented by discontinuous elements;
- simplified micro-modelling. The bricks are modelled as continuum elements, while the behaviour of the mortar joints and of the brick-mortar interface are lumped in discontinuous elements.

The main advantage of this method is the good representation of all failure mechanisms (especially under in-plane loading). However, computational time increase and sometimes convergence problems may stop the analysis when more accurated results are needed.

3. Proposed numerical model

In the present paper a variation of a macro-modelling approach was used to reproduce the in-plane stone masonry behaviour. Since the stones are stiffer and much stronger than the mortar, the stones could be modelled as rigid body elements in the FEM, while the mortar is represented by the continuum approach. As it is known, rigid bodies have just 3 DOF, this assumption allows the reduction of a great quantity of degree of freedoms (DOF) when modelling big structures with reduction of computational effort. The mortar is modelled considering a plastic-damage model developed by Lubliner et al. (1989) and later improved by Lee and Fenves (1998). This model is a continuum damaged model for quasi brittle materials under low confining pressures. The term brittle behaviour means that although the material has a low tensile strength, it shows inelastic deformation related to low strength values (Lourenco 1996; e.g. concrete, soil, cement mortar).

The plastic-damaged model is already implemented in Abaqus 6.9 Simulia (2009) under the name of concrete damaged plasticity model. The model assumes that failure of the material can be effectively modelled using its uniaxial tension, uniaxial compression and plasticity characteristics, such as the yield criterion, which determines whether the material shows elastic response at a particular state of stress; the flow rule, which defines the inelastic deformation that occurs when the material yields; and the hardening rule, which defines the way in which the inelastic deformations evolve. The failure is also characterized by the fracture energy (softening), which is the inelastic area below the stress-strain diagram (post peak behaviour) divided by the element characteristic length, h. This last value is used to avoid mesh dependency in the results, and is the length of a line across an element for a first-order element; or half of the same typical length for a second-order element.

Fig. 1 shows the uniaxial tension and compression behaviour of typical quasi-brittle materials. Different materials will have different strength and strain values. For tension loads, it follows an elastic behaviour up to the failure stress σ_{to}. Beyond this point the degradation due to the formation of micro-cracks is represented with a softening stress-strain curve. For compression loads the material response is elastic up to σ_{co}, similar to concrete material but with different strength value. As the material enters the plastic region, a hardening behaviour is imposed until the compression stress reaches σ_{cu}. Beyond this limit, a softening behaviour ensues that follows a parabolic shape. In case of reversal loading, the stress-strain curve may not follow the initial elastic stiffness because the descending part is affected by damage factors (dc, dt, Fig. 1), which could be calibrated from cyclic tests performed on the material. This stiffness reduction represents material degradation due to opening and closing of previously formed micro-cracks. Since the reproduced tests in this paper are monotonic, no damage factors were considered as part of the material properties.

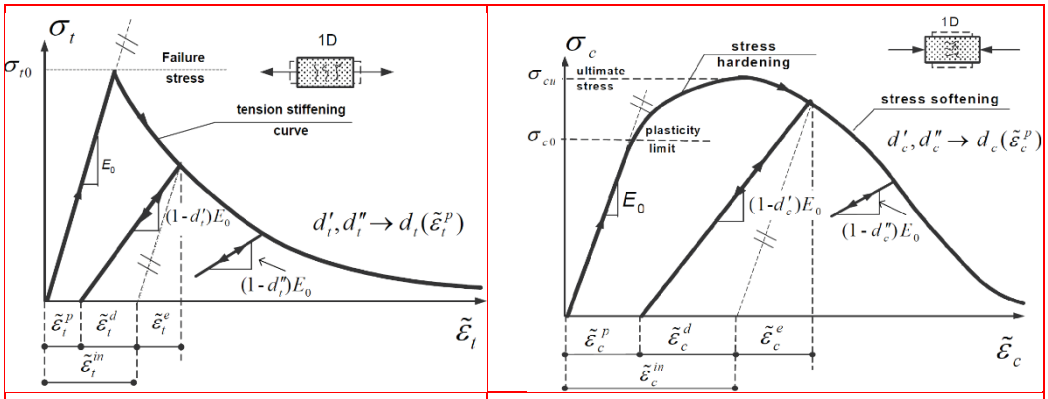

(a) tension behaviour (b) compression behaviour

Fig. 1 Response of concrete under tension and compression loads implemented in Abaqus for the concrete damaged plasticity model (modified from Wawrzynek and Cincio 2005).

The reduction of DOFs for the stones is suitable to save computational time when analysing other walls. Furthermore, this approximation will be useful for further parametric analyses to evaluate how the stone's quantity, dimension and disposition (geometric survey) could influence on the lateral capacity of walls; besides, authors believe that the length and pattern of the mortar layer have a great influence also on it. Therefore, if this simplify procedure is verified, then more analysis could be done to end on a general equation to predict the lateral resistance of stone walls taking into account all the preliminary variables.

4. Validation of the proposed simplified numerical approach

For the purpose of the present work, a diagonal compression test performed within the TREMA project (Technologies for the Reduction of seismic Effects on Architectural Buildings, Dolce et al. 2008) and shear compression tests performed by Vasconcelos (2005) are described hereafter. These two experimental studies were selected because other researchers have also used them to perform numerical modelling by using different FEM approaches (e.g. simplified micro-modelling) and FEM software (Betti et al. 2012). In this case, the work submitted here might also be useful as a comparison with the other numerical works.

4.1 Diagonal compression test

4.1.1. Description of the experimental test

Within the scope of the TREMA project (Technologies for the Reduction of seismic Effects on Architectural Buildings), experimental tests on irregular tuff masonry with low quality mortar (consisted on hydraulic lime, cement and sand) were performed at the University of Basilicata (Dolce et al. 2008). The wall's thickness consisted of two stone layers interconnected by the mortar (Fig. 2a). To characterize the mechanical properties in tension and compression of the mortar, 21 bending and 24 compression tests were performed. The first were tested on prismatic bars (160mmx160mmx40mm) while the last were tested on cubes of 40mm. Then, 3 diagonal compression tests (force controlled) were performed to compute the tensile strength of the masonry (labelled M1, M2 and

M3 with dimensions of 900 x 900 x 250 mm each, see Fig. 2). From the compression tests performed on the mortar, a mean value of 0.71 MPa with a COV of 0.22 was obtained. This low compression strength value represented the mortar deteriorated stage, typically found in historical stone masonry (Magenes et al. 2010, 2014). In the diagonal compression tests, before the application of the vertical load, a pre-compression load of 0.10, 0.15 and 0.20 MPa was applied to two opposite edges of specimens M1, M2 and M3, respectively (Fig. 2c), and was kept constant during the test. The vertical load was then applied within a force-controlled procedure up to collapse of the wall, which was characterized by diagonal cracking and crushing at the head wall. The maximum vertical force registered was 37.1 kN, 27.8 kN and 51.5 kN for M1, M2 and M3, respectively.

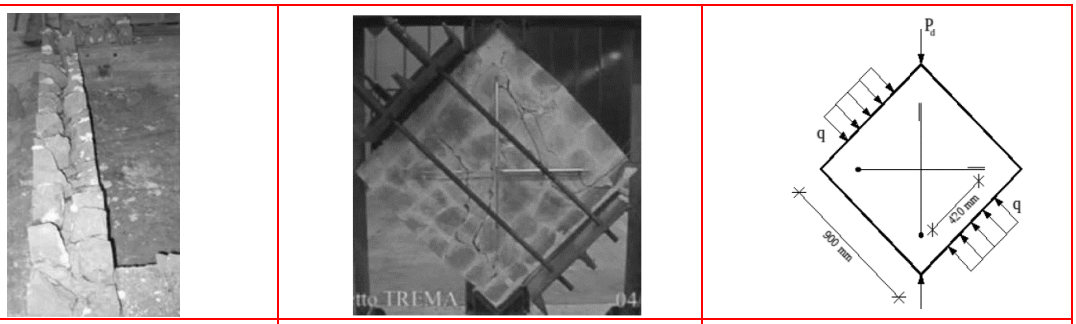

(a) stone wall pattern (b) diagonal compression test (c) test scheme

Fig. 2 Experimental test performed within TREMA (Dolce et al. 2008)

4.1.2 Description of the numerical modelling

The geometry of the diagonal compression models is shown in Figure 3a, which is the one corresponding to M1 with a pre-compression load oh 0.10 MPa. In all cases the surfaces (stone and mortar) were drawn for simplification in a CAD software and then exported to Abaqus. Steel elements were placed at the base, at the top, and at two edges of the masonry wall (see dark lines in Fig. 3a), the stones were represented by rigid body elements (using rigid body constraints) and the mortar by continuum elements. For the mesh, 4-node rectangular shell elements and 3-node triangular elements were used to represent the stone and mortar, respectively (Fig. 3b). The characteristic element length for the mortar was kept as close as possible to 21 mm to have at least 2 shell elements in the mortar layer.

The elastic material properties for the steel and mortar are given in Table 1. Although the stone elements were made rigid through a Rigid Body constraint, the FEM software needs some elastic properties as modulus of elasticity (E=50000 MPa) and Poisson's module (v= 0.20). The stone' specific weight was 16.7 E-06 N/mm^3.

From the experimental compression tests on mortar samples, a mean fc of 0.71 MPa was computed with a coefficient of variation of 0.22 MPa; while the E was initially estimated as 900 MPa according to Dolce et al. (2008). Therefore, also in the elastic range some material properties needed to be calibrated to match the initial stiffness as in other researchers (Betti et al. 2012). The other inelastic material properties given in Table 2 were also calibrated to match the numerical response and failure pattern with the observed post peak experimental behaviour. The calibration process of these properties was carried out varying one by one each of the material parameters. For example, the tensile strength was estimated first as 10% of fc and then it was reduced until get a

reasonable numerical result. The fracture energy values were kept low, starting from values recommended by Lourenco (1996).

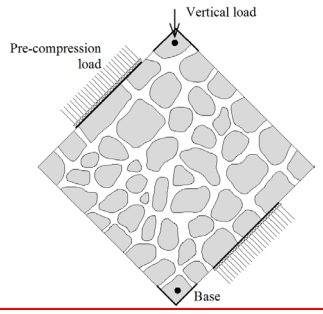

(a) sketch of the diagonal compression test

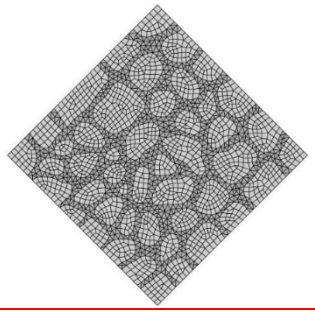

(b) mesh of the numerical model

Fig. 3 Diagonal compression test (900x900x250mm)

Table 1 Elastic material properties for the steel and mortar

Steel		Mortar		
E (MPa)	*v*	*E (MPa)*	*v*	γ_m *(N/mm³)*
200 000	0.25	950	0.20	16.0 E-06

Table 2 Mortar material properties used for the plasticity-damage model

Tension (softening)		Compression (hardening/softening)			
f_t *(N/mm²)*	G_{ft} *(N/mm)*	f_c *(N/mm²)*	f_{ci} *(N/mm²)*	G_{fc} *(N/mm)*	ε_p *(mm/mm)*
0.04	0.001	0.50	0.10	0.300	0.004

4.1.3 Numerical analysis and results

For the analysis the boundary conditions (BC) and the loading sequence were those used during the experimental test. Regarding the BC, horizontal and vertical degrees of freedoms (DOF) at the wall base were restrained, while at the top part just the horizontal one was restrained. Then, pre-compression load was applied at the two edges (steel plates) and kept constant during all the analysis. Finally, the vertical load was then applied at the wall top up to wall failure. Nonlinear geometrical effects were also considered in the model. The numerical analysis followed a full Newton-Raphson iterative procedure and an automatic stabilization was selected for the convergence criterion, with a specified dissipated energy fraction of 0.0001 and an adaptive stabilization with maximum ratio of stabilization to strain energy of 0.05. These values were selected to obtain reasonable failure patterns in the model without loss of accuracy.

The results showed that the numerical model reproduced fairly well the general response of the wall, the stress distribution and the failure pattern of the experimental test. In the Force-Displacement curves (F-D) shown in Fig. 4 the reaction due to self-weight was not considered, therefore the contribution to the vertical force was due to the pre-compression and vertical loads only. The assumption of rigid body elements for the stones seems to be acceptable to represent the structural response as most of the deformation and inelasticity developed in the mortar. No cracks were visible in the stones in the test. It is important to note that the initial part of the F-D curve was

controlled by the modulus of elasticity of the mortar, whose numerical value was calibrated through a parametric analysis. When the stresses exceeded the maximum tensile strength, cracks started forming, thus changing the slope of the F-D curve. At 0.30 mm displacement, crushing was observed at the top of the wall due to compression stress concentration in the mortar. This compression crushing failure controlled the damage sequence. As the vertical load increased, more diffuse tensile cracking appeared in the mortar, especially in the top section of the wall. At 0.50 mm top displacement, 3 (almost vertical) cracking paths became clearly visible through the masonry wall. In the experimental test these diagonal quasi-vertical cracks splitted the wall into almost three blocks (see Fig. 2b). In the numerical model, the compression stress in the wall center increased and more crushing was observed until no convergence of the model, corresponding to failure. In the F-D curve 3 zones are identified: the initial elastic zone is controlled by the mortar elastic modulus; after cracking in the mortar started and propagated, the slope of the F-D curve changes and the tensile fracture energy allows stress re-distribution in the wall; finally, the compression stress concentration at the wall top defines the maximum vertical force and the subsequent wall collapse.

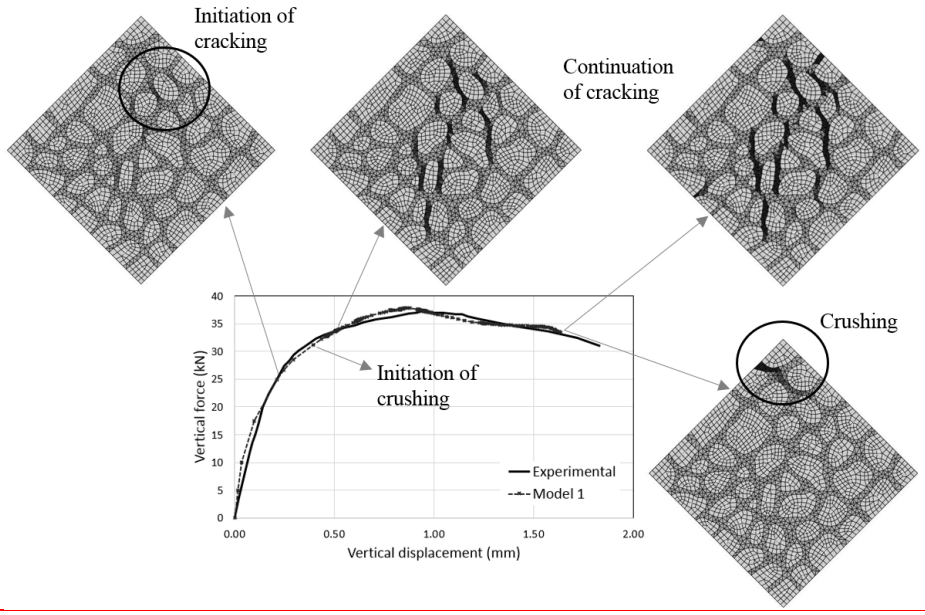

Fig. 4 Comparison of the experimental and numerical Force-Displacement curve and evolution of damage during the diagonal compression test

4.2 Shear compression tests

4.2.1. Description of the experimental test

Vasconcelos (2005) carried out a research programme at the University of Minho for the experimental evaluation of the in-plane seismic performance and failure pattern of ancient stone masonry without and with bonding mortar (in single leaf walls). Three masonry panel typologies were studied: dry-stone masonry (WS), irregular stone masonry (WI) and rubble stone masonry (WR). A total of 10 WS, 7 WI and 7 WR specimens, all with dimensions 1000 x 1200 x 200 mm,

were built. Fig. 5 shows a sketch of a rubble masonry wall. Each panel was subjected to a pre-compression vertical load followed by a cyclic horizontal top displacement. The pre-compression values were 0.50, 0.875 and 1.25 MPa, and allowed to study the influence of axial vertical stresses due to gravity loads. The mortar compression strength for WI and WR was around 3.0 MPa. The adopted dimensions for the walls and stone units were about 1:3 scale for single leaf walls found in northern Portugal. Later, Senthivel and Lourenço (2009) numerically reproduced this test.

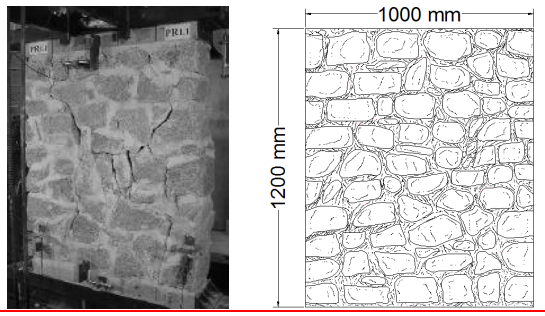

Fig. 5 Masonry wall sample studied by Vasconcelos (2005)

4.2.2 Description of the numerical modelling

The tests performed by Vasconcelos (2005) for rubble stone masonry (labelled WR) are studied here through the comparison with numerical analyses. In that research two stone walls were tested for each pre-compressional level: WR1-100 and WR2-100, WR1-175 and WR2-175, and WR1-250 and WR2-250, in total 6 specimens. As in the previously described diagonal compression test, the geometry was drawn in a CAD software and then exported to the FEM software. A scheme of the test is shown in Fig. 6a. For the mesh, 4-node rectangular shell elements and 3-node triangular elements were used to represent the stone and the mortar, respectively (Fig. 6b). The characteristic element length for the mortar elements was kept as close as possible to 20 mm to have at least two shell elements in the mortar layer. For the stones, first, an elastic material with modulus of elasticity E=202 000 MPa and Poisson's ratio v= 0.20 was specified as in Senthivel and Lourenco (2009), then a Rigid Body constrain was applied to each element. The stone specific weight is 26 E-06 N/mm^3. The material properties used for the stone and mortar were based on the values reported by Senthivel and Lourenco (2009) and Vasconcelos (2005, Table 3 and Table 4). For the mortar, the modulus of elasticity was initially computed as the joint stiffness described by Senthivel and Lourenco (2009), kn= 2 MPa/mm, times the mortar thickness. However, not all the required information was available, especially the inelastic one. For example, the fracture energy in tension G_{ft} and compression G_{fc} for the plastic-damage model of the mortar needed to be calibrated based on parametric studies but starting from values suggested by Vasconcelos (2005). The most important issue in this case was to keep an exponential softening behaviour for tension and parabolic shape for compression (Lourenco 1996).

The calibration process was performed varying each of these fracture energies one at a time and running the analyses until attainment of an acceptable agreement between numerical and experimental Force vs Displacement curve and failure pattern of the wall. While the experimental test considered a pseudo-static cyclic displacement history, only the envelope of the cyclic response was reproduced in the numerical analyses. The calibration process (definition of all material

properties) was performed based on the geometry and experimental results of the wall with a pre-compression load of 0.875 MPa subjected to a horizontal load applied from left to right.

Table 3 Mortar elastic material properties

Mortar		
E (MPa)	v	γ_m (N/mm^3)
115	0.20	20.0 E-06

Table 4 Mortar material properties used for the plasticity-damage model

Tension (softening)		Compression (hardening/softening)			
f_t (N/mm^2)	G_{ft} (N/mm)	f_c (N/mm^2)	f_{ci} (N/mm^2)	G_{fc} (N/mm)	ε_p (mm/mm)
0.05	0.01	2.50	2.30	4.900	0.0175

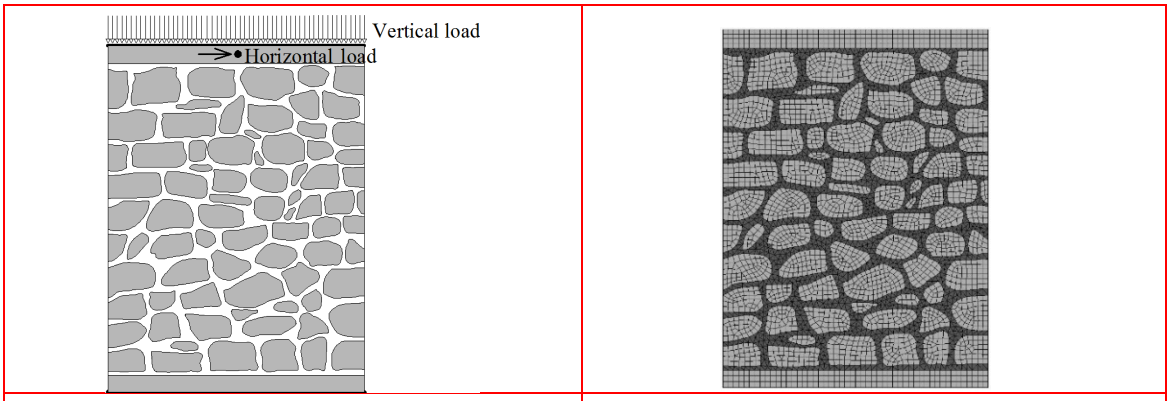

(a) sketch of the test (b) mesh of the numerical model

Fig. 6 Shear compression test

4.2.3 Numerical analysis and results

Since the rubble stone wall is not symmetric, two analyses were carried out with the previous calibrated material properties, one considering a horizontal force acting from left to right, the other with the load applied right to left. The analysis considered a full Newton-Raphson iterative procedure and an automatic stabilization was selected for the convergence criterion, with a specified dissipated energy fraction of 0.0002, 0.002 and 0.01 for the gravity, pre-compression and displacement loads, respectively, and an adaptive stabilization with maximum ratio of stabilization to strain energy of 0.05 for gravity and pre-compression loads. The comparison of the experimental and numerical Force vs Displacement responses is shown in Fig. 7. During the load application the first regions to exceed the tensile strength were the horizontal (heel and toe) edges of the wall. Later, cracks appeared at the centre wall following a diagonal path along the mortar. The progressive stiffness reduction in the numerical curves from Fig. 7 was due to cracking in the wall. Diagonal shear failure occurred when the diagonal tensile stress resulting from the compression shear state exceeds the splitting tensile strength of the mortar. The maximum lateral capacity and post peak behaviour of the curves in Fig. 7 was not only influenced by the cracking formation, but also by the mortar compressive strength and by the compression fracture energy. Greater values of the

compressive fracture energy lead to an increment of the displacement pseudo-ductility of the stone wall till collapse.

Senthivel and Lourenço (2009) numerically reproduced the tests performed by Vasconcelos (2005) using a simplified micro-modelling approach (2D nonlinear finite element analysis). The stone units were modelled using an eight node continuum plane stress elements with full Gauss integration. The joints and unit joint interfaces were modelled using six node zero thickness line interface elements with Lobatto integration. They were able to reproduce the model deformation characteristics, such as load-displacement envelope diagrams and failure modes. In Fig. 7, the numerical results by Senthivel and Lourenço (2009) are also reported here and labelled S&L 2009.

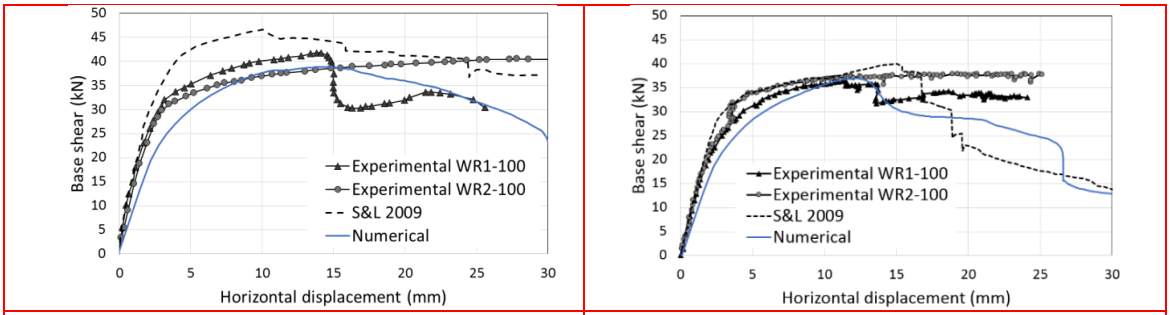

loading from left to right | loading from right to left

(a) Pre-compression load 0.5 MPa (related to 100 kN)

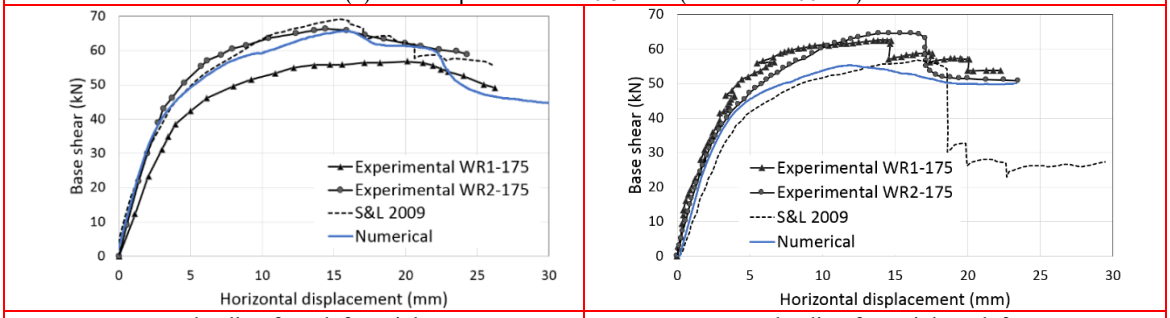

loading from left to right | loading from right to left

(b) Pre-compression load 0.875 MPa (related to 175 kN)

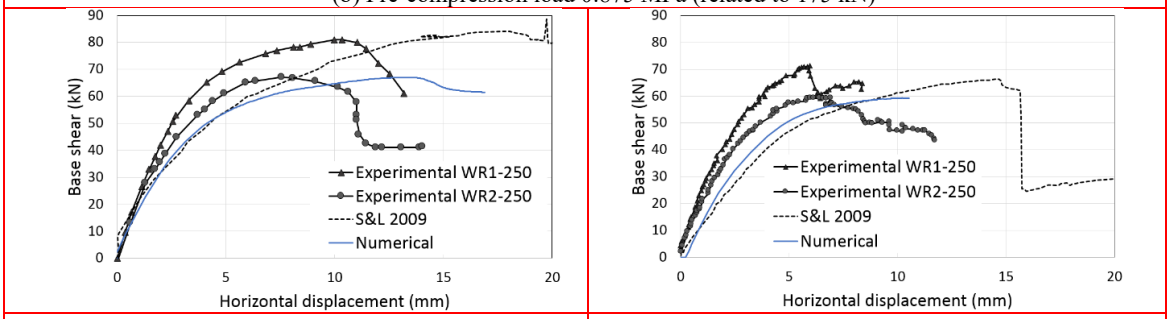

loading from left to right | loading from right to left

(c) Pre--compression load 1.25 MPa (related to 250 kN)

Fig. 7 Comparison of numerical and experimental Force vs Displacement curves of rubble masonry

The numerical failure patterns obtained in this work are similar to the ones reported by Senthivel

and Lourenço (2009), see Fig. 8-10. However, the proposed model does not allow the physical separation of stone units. Mainly, the numerical model stopped due to diagonal cracking at the wall mid-height and tensional failure on the heel and toe zones due to high compression stresses. The acceptable agreement in terms of overall force-displacement responses and observed damage formation and progression documented in Fig.8 - 10 show the good performance of the numerical model used in this study and confirm that a rubble masonry with strong stone and weak mortar can be effectively modelled with the proposed model that assumes the stones rigid and ascribes all deformability and inelasticity to the mortar.

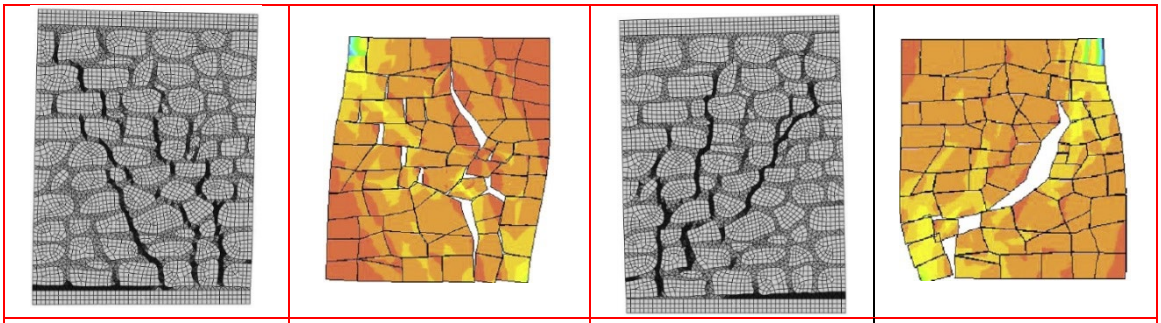

(a) Load x+	(b) Load x+ S&L2009	(a) Load x-	(b) Load x- S&L2009

Fig. 8 Numerical failure pattern vs experimental pattern. Pre-compression load 0.5 MPa

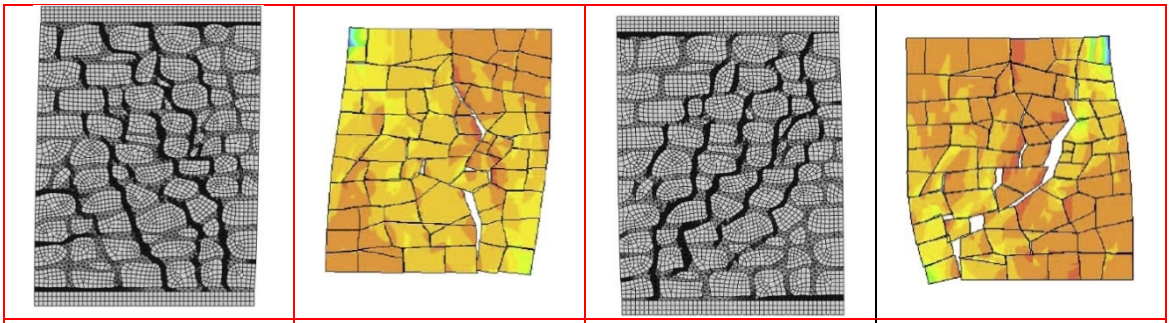

(a) Load x+	(b) Load x+ S&L2009	(a) Load x-	(b) Load x- S&L2009

Fig. 9 Numerical failure pattern vs experimental pattern. Pre-compression load 0.875 MPa

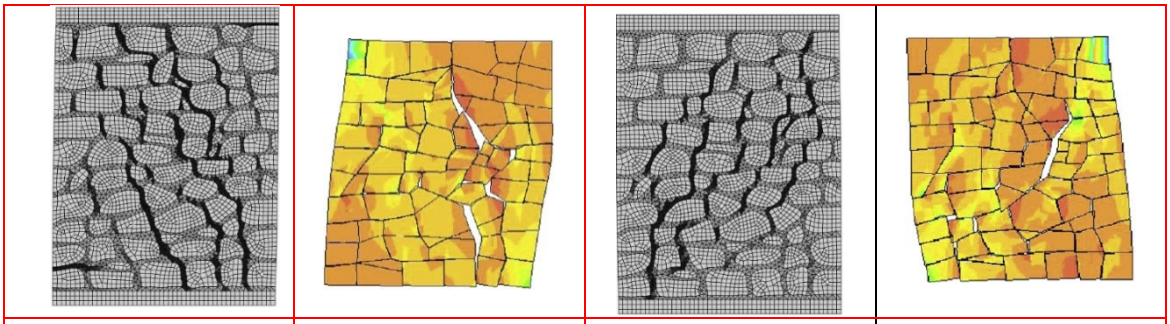

(a) Load x+	(b) Load x+ S&L2009	(a) Load x-	(b) Load x- S&L2009

Fig. 10 Numerical failure pattern vs experimental pattern. Pre-compression load 1.25 MPa

5. Influence of the stone's quantity and of the stone's arrangement on stone's wall behaviour

5.1 Description of the models

To evaluate the influence of the stone's quantity and arrangement on the lateral strength, and to verify the efficiency of the numerical approach shown here, six stone panels (Fig. 11) were created with dimensions 900x900x250 mm. Panel patterns M2, M3, M4, M5, and M6 were obtained from real Italian stone wall patterns. Panel M1 represents a regular stone masonry with the objective of comparing its behaviour with the other, more irregular patterns.

All panels have stone material between 72% to 80% of the total wall area; however, having the same quantity of stone material does not imply having the same quantity of stone units. For example, the number of stone units in panels M1 to M6 is 26, 92, 94, 122, 79 and 74, respectively.

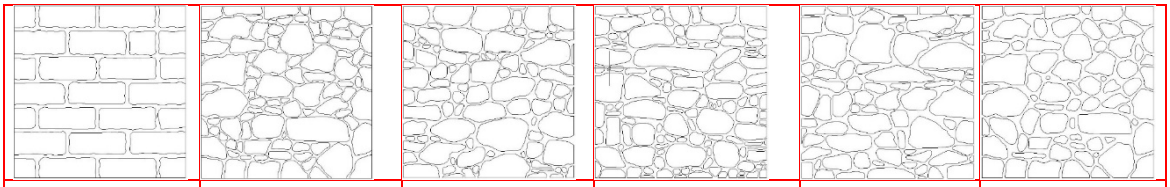

Fig. 11 Pattern of stone masonry panels

5.2 Numerical analyses and results

The stone walls were subjected to a shear compression test. After imposing gravitational loading, a vertical compression stress of 0.10 MPa was kept constant at the panel top. Finally, a top lateral displacement was imposed up to the wall collapse. Two analyses were carried out for each panel, one considering the horizontal load applied left to right, and the other right to left, simulating two independent pushover tests. The material properties were those reported in Table 1 and Table 2. The analyses considered a full Newton-Raphson iterative procedure and an automatic stabilization was selected for the convergence criterion, with a specified dissipated energy fraction of 0.0002, 0.002 and 0.01 for the gravity, pre-compression and displacement load, respectively, and an adaptive stabilization with maximum ratio of stabilization to strain energy of 0.05 for gravity and pre-compression loads.

Similarly, to the previous models, the first zones to exceed the mortar tensile strength were the horizontal top and bottom parts of the walls; for larger lateral displacements, diagonal cracks started to appear from the centre to the corners. Due to length limitation, just the Force-Displacement curves and failure patterns of loading from right to left are shown in Fig. 12. Dark zones indicate the complete loss of tensile strength in the mortar. The stone's distribution has an influence on the shear capacity of the panel. A regular stone distribution leads to an increment in the lateral strength but with a more brittle behaviour, as can be seen for M1. This is basically due to the fairly continuous cracking pattern along the wall diagonal. In contrast, a panel with more irregular stone units will have less shear capacity, but a more ductile response since the mortar does not follow a continuous path: the tensile cracking does not necessarily concentrated along the diagonal and tends to be smeared.

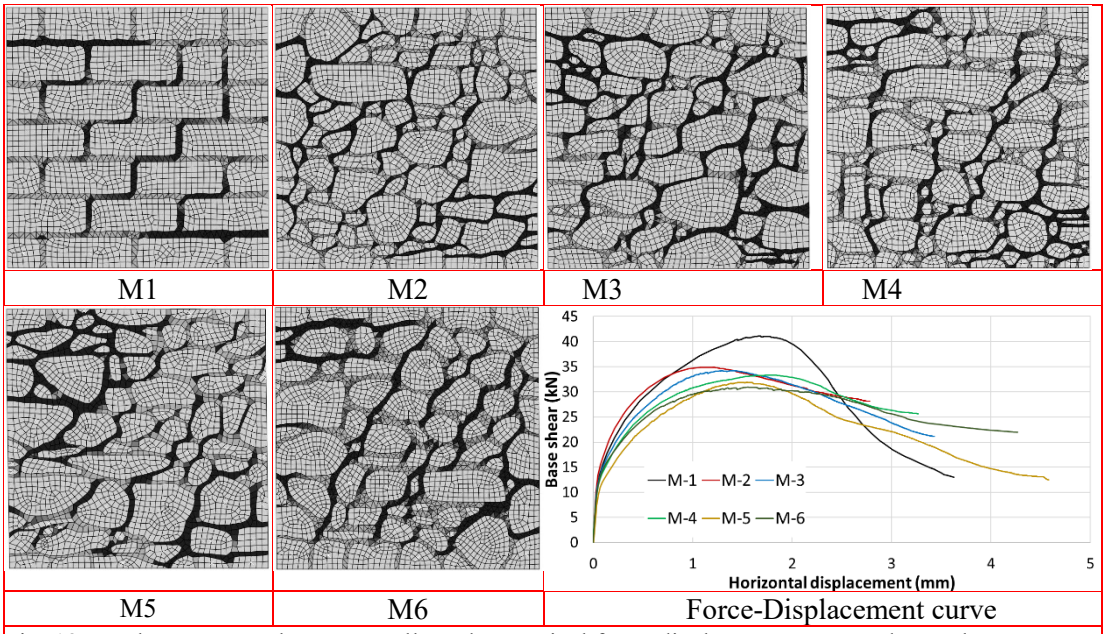

Fig. 12 Crack pattern on the stone walls and numerical force-displacement curves due to the horizontal load applied right to left

6. Conclusions

This paper investigates a simplified methodology for the fast prediction of the in-plane behaviour of stone walls with a uniform wall thickness. It was experimentally seen that the seismic behaviour of stone walls is almost entirely controlled by the mortar and the connection between the different stone leaves. Therefore, within the finite element method (FEM) the proposed methodology represents the mortar by a plastic-damage material with stiffness degradation and the stones as rigid bodies. This approach allows the reduction of the number of DOFs in the analysis, consequently saving computational time.

The validation of the methodology was carried out by replicating numerically two experimental tests performed on rubble single-leaf stone walls: one is a diagonal compression test and the other a shear compression test. The material properties (specifically for the mortar) were calibrated based on experimental data and the global response of the stone wall to match the Force vs Displacement curve and the observed damage pattern. During the calibration and numerical analyses, it was observed that the mortar tension and compression strengths were the two most important parameters for a good correlation between numerical and experimental results.

For the diagonal compression tests it was observed that crushing at the wall top (close to the load application zone) influenced the maximum capacity of the wall. In the shear compression test the heel and toe zones were subjected to high compression stresses. However, the progressive stiffness reduction in the Force vs Displacement curves was mainly controlled by the cracking process that started at the wall mid-height and expanded diagonally to the wall corners.

Comparing all Force vs Displacement curves, it seems to have an acceptable agreement with the experimental ones in most of the cases. However, a variation is allowed since the numerical model is just an approximation of the real behaviour. Furthermore, two similar real walls subjected to

lateral forces may vary its maximum lateral resistance depending on the mortar path and crack initiation; therefore, the arrangement of the stone units inside the wall has although an influence on the crack propagation. The results of the numerical models validates the assumption that the stone units could be treated as rigid bodies while mortar should be modelled as a non-linear element with limits in its tensile and compressive strength values.

To evaluate how the stone wall's response is affected by the quantity, dimension and distribution of stone units, 6 additional numerical models were replicated from Italian constructions. The results of numerical tests on these models showed that a uniform distribution of stone units allows a better confinement of the mortar material, and with that an increase on the wall capacity by 20%. If the wall is composed of many small stone units, cracking is more diffused along the mortar and less regular, resulting in a lower strength capacity but in an increase in displacement ductility.

The acceptable agreement between the numerical and experimental tests shows that the proposed methodology is quite promising. The method is computationally efficient because it saves computational time and can be easily extended to three-dimensional wall models and to study large structures.

References

Abaqus 6.9 SIMULIA. (2009), *Abaqus/CAE Extended Funcionality EF2, Manual*, Dassault Systemss Corporation, Providence, RI, USA.

Betti M, Bartoli G, Corazzi R, KovacevicV (2012). Strumenti Open Source per l'ingegneria strutturale. Modellazione meccanica non lineare di edifici in muratura. Bollettino degli Ingegneri, Collegio Ingegneri della Toscana, LX(12), pp 3–15 (in Italian)

Binda, L., Pina-Henriques, J., Anzani, A., Fontana, A. and Lourenço, P. (2006), "A contribution for the understanding of load-transfer mechanisms in multi-leaf masonry walls: Testing and modelling". *Engineering Structures*, **28**(8), 1132–1148.

Cattari, S. and Lagomarsino, S. (2013), "Seismic assessment of mixed masonry-reinforced concrete buildings by non-linear static analyses", *Earthquake and Structures*, **4**(3), 241-264.

Corradi, M., Borri, A. and Vignoli, A. (2003), "Experimental study on the determination of strength of masonry walls". *Construction and Building Materials*, **17**, 325-333.

Doğangün, A. and Sezen, H. (2012), "Seismic vulnerability and preservation of historical masonry monumental structures", *Earthquake and Structures*, **3**(1), 83-95.

Dolce, M., Ponzo, F.C., Goretti, A., Moroni, C., Giordano, F., de Canio, G., and Marnetto, R. (2008), "3D dynamic tests on 2/3 scale masonry buildings retrofitted with different systems". *In Proceedings of the 14th World Conference on Earthquake Engineering*, Beijing, China.

Frumento, S. (2007), "Identificazione dei parametri di risposta a taglio di pannelli murari attraverso la prova di compressione diagonale (in Italian)". PhD thesis, DICAT Università degli Studi di Genova, Genova, Italy.

Gardin, B. (2007), "Diagnosi delle murature storiche mediante procedure debolmente distruttive: problematiche nell'uso dei martinetti piatti (in Italian)", Master thesis, University of Padua, Padua, Italy.

Gautam, D., Rodrigues, H., Bhetwal, K., Neupane, P., and Sanada Y. (2016), "Common structural and constructions deficiencies of Nepalese buildings", *Innovative Infrastructure Solutions Journal*,1(1), 1-18.

Graziotti, F., Magenes, G., and Penna, A. (2016), *Experimental campaign on double-leaf stone masonry specimens at the University of Pavia and EUCENTRE Pavia*. Experimental researches on the seismic behaviour of masonry spandrels: an international perspective, Chapter: 2, Publisher: EUCENTRE Press, Editors: Nicola Augenti, Francesco Graziotti, Guido Magenes, Fulvio Parisi.

Karantoni, F., Tsionis, G. Lyrantzaki, F. and Fardis, M.N. (2014). "Seismic fragility of regular masonry buildings for in-plane and out-of-plane failure", *Earthquake and Structures*, **6**(6), 689-713.

Lagomarsino, S., Penna, A., Galasco, A. and Cattari, S. (2013), "TREMURI program: An equivalent frame model for the nonlinear seismic analysis of masonry buildings". *Engineering Structures*, 56, 1787-1799

Magenes, G., Penna, A., Galasco, A., and Rota, M. (2010), "Experimental characterization of stone masonry mechanical properties". *In Proceedings of the 8th International Masonry Conference*, Dresden, Germany.

Magenes G., Penna A., Senaldi I., Rota M. , Galasco A. (2014), "Shaking Table Test of a Strengthened Full-Scale Stone Masonry Building with Flexible Diaphragms", *International Journal of Architectural Heritage*, Taylor and Francis, **8**(3), 349-375.

Milosevic, J., Lopes, M., Sousa, A. and Bento, R. 2013a. Testing and modelling the diagonal tension strength of rubble stone masonry panels. Engineering Structures, 52: 581-591

Milosevic, J., A. Gago, M. Lopes, R. Bento. (2013b), "Experimental assessment of shear strength parameters on rubble stone masonry specimens", Construction and Building Materials 47, 1372-1380 doi: 669 10.1016/j.conbuildmat.2013.06.036

Oliveira, D. and Lourenço, P. B. (2006), "Experimental behaviour of three-leaf stone masonry walls". *In Proceeding of The construction aspects of built heritage protection*, Dubrovnik, Croatia, 356–362.

Oliveira, D., Silva, R.A., Garbin, E., Lourenço, P.B. (2012), "Strengthening of three-leaf stone masonry walls: an experimental research". *Materials and Structures*, **45**, 1259-1276

Pagnini, L.C., Romeu, V., Lagomarsino, S. and Varum, H. (2011), "A mechanical model for the seismic Vulnerability assessment of old masonry buildings", *Earthquake and Structures*, **2**(1), 25-42.

Pelà, L., Cervera, M., and Roca, P. (2013), "An orthotropic damage model for the analysis of masonry structures". *Construction and Building Materials*, **41**, 957-967.

Penna, A., Senaldi, I., Galasco A., and Magenes, G. (2016), "Numerical Simulation Of Shaking Table Tests On Full-Scale Stone Masonry Buildings", *International Journal of Architectural Heritage*, 10(2,3), 146-163.

Roca, P., Molins, C. and Marí, A. (2005). "Strength Capacity of Masonry Wall Structures by the Equivalent Frame Method". *Journal of Structural Engineering*, Vol. 131(10). Technical paper.

Seker, B. S., Cakir, F., Doğangün, A., Uysal, H. (2014), " Investigation of the structural performance of a masonry domed mosque by experimental tests and numerical analysis", *Earthquake and Structures*, **6**(4), 335-350.

Senthivel, R. and Lourenço, P.B. (2009), "Finite element modelling of deformation characteristics of historical stone masonry shear walls". *Engineering Structures*, **31**, 1930-1943.

Spacone, E. and Camata G. (2016), *Esecuzione di prove non destruttive in situ e di laboratorio distruttive su provini e modelli (in Italian)*. Convenzione di ricerca sulle malte idreuliche nell'ambito del POR FESR Abruzzo 2007-2013. Universitá degli Studi "Gabriele d'Annunzio", Chieti-Pescara, Italy.

Tarque, N., Camata, G., Spacone, E., Varum, H. and Blondet, M. (2014), "Nonlinear Dynamic Analysis of a Full-Scale Unreinforced Adobe Model". *Earthquake Spectra*, **30**(4), 1643-1661.

Ural, A. (2013), "19th May 2011 Simav (Kutahya) earthquake and response of masonry Halil Aga Mosque", *Earthquake and Structures*, **4**(6), 671-683.

Valluzi, M.R., da Porto, F. and Modena, C. (2001), *Behaviour of multi-leaf stone masonry walls strengthened by different intervention techniques*, Historical Constructions, P.B. Lourenço and P. Roca (Eds.), pp. 1026-1032, Guimaraes, Portugal.

Vasconcelos, G. (2005), "Experimental investigations on the mechanics of stone masonry: Characterization of granites and behaviour of ancient masonry shear walls", Ph.D. thesis, University of Minho, Guimaraes, Portugal.

Vasconcelos, G. and Lourenço, P. (2009), "Experimental characterization of stone masonry in shear and compression". *Construction and Building Materials*, **23**(11), 3337–3345.

Vintzileou, E., Mouzakis, C., Adami, C. and Karapita, L. (2015), "Seismic behavior of three-leaf stone masonry buildings before and after interventions: Shaking table tests on a two-storey masonry model", *Bull Earthquake Eng*, **13**(10), 3107-3133.